

Article

Optimization of the CO₂ Liquefaction Process-Performance Study with Varying Ambient Temperature

Steven Jackson *  and Eivind Brodal

UiT-Norges Arktiske Universitetet, Postboks 6050 Langnes, 9037 Tromsø, Norway; eivind.brodal@uit.no

* Correspondence: steve.jackson@uit.no

Received: 8 October 2019; Accepted: 19 October 2019; Published: 22 October 2019



Abstract: In carbon capture utilization and storage (CCUS) projects, the transportation of CO₂ by ship can be an attractive alternative to transportation using a pipeline, particularly when the distance between the source and usage or storage location is large. However, a challenge associated with this approach is that the energy consumption of the liquefaction process can be significant, which makes the selection of an energy-efficient design an important factor in the minimization of operating costs. Since the liquefaction process operates at low temperature, its energy consumption varies with ambient temperature, which influences the trade-off point between different liquefaction process designs. A consistent set of data showing the relationship between energy consumption and cooling temperature is therefore useful in the CCUS system modelling. This study addresses this issue by modelling the performance of a variety of CO₂ liquefaction processes across a range of ambient temperatures applying a methodical approach for the optimization of process operating parameters. The findings comprise a set of data for the minimum energy consumption cases. The main conclusions of this study are that an open-cycle CO₂ process will offer lowest energy consumption below 20 °C cooling temperature and that over the cooling temperature range 15 to 50 °C, the minimum energy consumption for all liquefaction process rises by around 40%.

Keywords: CO₂; liquefaction; CCUS; optimization; ambient temperature

1. Introduction

Carbon capture utilization and storage (CCUS) refers to a wide-ranging set of techniques that can be used to mitigate anthropogenic CO₂ emissions. Utilization methods include enhanced oil recovery (EOR), enhanced coal bed methane (ECBM), mineral carbonation, biological algae cultivation, conversion into synthesized fuels and chemicals feedstock. A recent review of the patents being published in field of CCUS concludes that, although the most patents concern utilization of CO₂ in the production of fuels and chemicals, there are also a large number of patents published on algae cultivation, EOR, and ECBM [1].

The aim of many CCUS technologies is the re-use of CO₂ emissions in the location where they are generated thereby eliminating any need for transportation and driving the development of a more circular economy. However, in the case of EOR and ECBM, a transportation step is usually needed, which can represent a significant challenge to the implementation of these types of CCUS projects [2,3]. Although there exists around 8000 km of CO₂ pipeline in the world today, it is estimated that over 200,000 km of pipeline will be required by 2050 [4]. In addition, as the variety of CO₂ sources considered in CCUS projects becomes more diverse, the challenges associated with transporting CO₂ can be expected to multiply.

The transportation of CO₂ by sea on a small scale has been a commercial practice in Europe for several years, where ships are used to transport food-quality CO₂ from production plants to coastal distribution terminals [5]. The current commercial vessel sizes vary between 1000 and 1500 m³ and the transport pressure is in the range 14–20 bara [6]. Although the use of shipping in many CCUS projects would require a considerable scale-up in transport capacity, there are no technical barriers and shipping has long been identified as a potential option for the long-distance transport of CO₂. The IPCC special report on CCS [5], for example, identifies shipping as the lowest cost option for distances over 1700 km. Other studies such as Mallon et al. [7] and Jakobsen et al. [8] have found that the trade-off distance for shipping could be much lower. As a result, shipping of CO₂ is a standard feature in the modelling of CCS transportation networks and a significant number of studies have been made into the technical and commercial aspects of the liquefaction processes required, for example, the studies of Mitsubishi in 2004 [9], Jordal et al. in 2007 [10], and Roussanly et al. in 2014 [11].

When transporting CO₂ in ships, the energy consumption of the liquefaction process is significant, implying high operating costs. As a result, many studies have considered the design of the liquefaction process, particularly with a focus on reducing energy consumption. Hegerland [6] states that “in principle, there are two process alternatives” and goes on to suggest that when low temperature cooling water is available, CO₂ should be used directly as a cooling medium, but above a trade-off temperature, an in-direct ammonia (NH₃) refrigeration process becomes the best option. Subsequent studies have considered the selection of the optimal process flow scheme for the liquefaction of CO₂ in more detail. Although the majority of work is focused on either open cycle CO₂ processes or closed cycle NH₃ refrigeration processes, others have also studied more novel approaches such as the use of absorption refrigeration [12], cascade refrigeration [13], and the application of turbo expanders [14]. Some have also compared a broad range of schemes. Alabdulkarem et al. [13], for example, compares simple refrigeration schemes, cascade refrigeration schemes, and absorption refrigeration schemes using waste heat. Most studies, however, focus on the performance of one or two schemes and one set of operating conditions.

In addition to the selection of the process flow scheme, the chosen CO₂ transport pressure represents an important operating parameter for the liquefaction process. Hegerland [6] states that “to reduce investment costs of storage and ship tanks, it is required to operate as close to the triple point of 5.17 bara and –56.6 °C as practically feasible.” Aspelund et al. [15] and Lee et al. [16] looked at 6.5 bara transportation pressure based on the design of current commercial CO₂ transportation by ship and also follow the assumption that the larger vessels used for CCS would operate at lower pressures. Decarre et al. [17] compared liquefaction at 7 bara and 15 bara, finding that transportation at 15 bara offers both lowest cost and lowest energy consumption. Seo et al. over the course of two papers, [18] and [19], also studied the optimum liquefaction pressure conditions finding that the overall cost was lowest for 15 bara cases. More generally, both Seo et al. [19], Alabdulkarem et al. [13], and Jackson et al. [20] found the optimum liquefaction pressure for the transportation of CO₂ by pipeline to be around 50 bara, which is well above the practical limits for ship-based transport.

In addition to Hegerland et al. [6], Lee et al. [21] also investigated the relationship between cooling temperature and liquefaction process performance. However, both of these studies only consider liquefaction at low pressure and Lee et al. limit their study to the performance of open cycle CO₂ processes. The approach taken by this study is, therefore, novel in as much as it studies how minimum energy consumption for a variety of different CO₂ liquefaction process, operating at up to 15 bara, varies with cooling temperature. The results of this study are used to identify the trade-off point in terms of minimum energy consumption for NH₃ and CO₂-based systems. The main aim of this study is to present a consistent set of data for the variation in the minimum energy consumption of CO₂ liquefaction across a range of ambient temperatures that can be used in the modelling a CCUS transportation systems.

2. Materials and Methods

The study method is set out below in two parts: first, a general description of the study approach is made, which breaks the methods employed into five steps; second, a more detailed description is presented for each of the five steps.

2.1. General Description

To begin with, a survey of previous studies was made to help identify the full range of possible process flow schemes available for the liquefaction process. Based on a review of the studies mentioned in the introduction, three were selected as the basis for further work that covered all of the principle flow scheme alternatives: Alabdulkarem et al. [13], Seo et al. [18], and Øi et al. [14]. From these three studies, four “base” flow schemes were then selected.

In the first phase of the modelling work, each of the four “base” schemes were modelled using the parameters from the study to which they belong. This exercise provided both a verification of the modelling approach and the correct interpretation of the design intent of each scheme. The performance of each scheme was then compared using a new common set of “base” parameters to allow an unambiguous comparison of the performance of each process. Importantly, the operating parameters for each of the process schemes were optimized with the “base” parameters for minimum energy consumption. After this, an additional set of process flow schemes was developed based on the most promising features from the schemes already modelled and finally, the performance of all schemes was compared to identify the best performing schemes to be use in the final phase of modelling work.

In the final phase of work, the performance of the best performing schemes was investigated over a range of ambient temperature conditions. At each temperature condition the operating parameters of each scheme were optimized to provide an accurate reflection of how performance varies with ambient temperature.

The method described above is summarized below as a five-step process. More detail on each of the individual steps is then presented below under separate sub-headings.

1. Selection of “base” flow schemes and parameters
2. Validation of the modelling basis
3. Optimization and comparison of the “base” schemes
4. Development and selection of the study basis
5. Performance variation with cooling temperature

2.2. Selection of “Base” Flow Schemes and Parameters

The “base” schemes selected for this study were: a CO₂-NH₃ closed-loop refrigerant cascade scheme as Case 1 from Alabdulkarem et al. [13]; an NH₃ based refrigeration scheme as Case 2 from Seo et al. [18] and as Case 3 from Øi et al. [14]; and an open-cycle CO₂ scheme as Case 4, also from Øi et al. [14]. A process flow diagram for each of these schemes is presented in Figure 1.

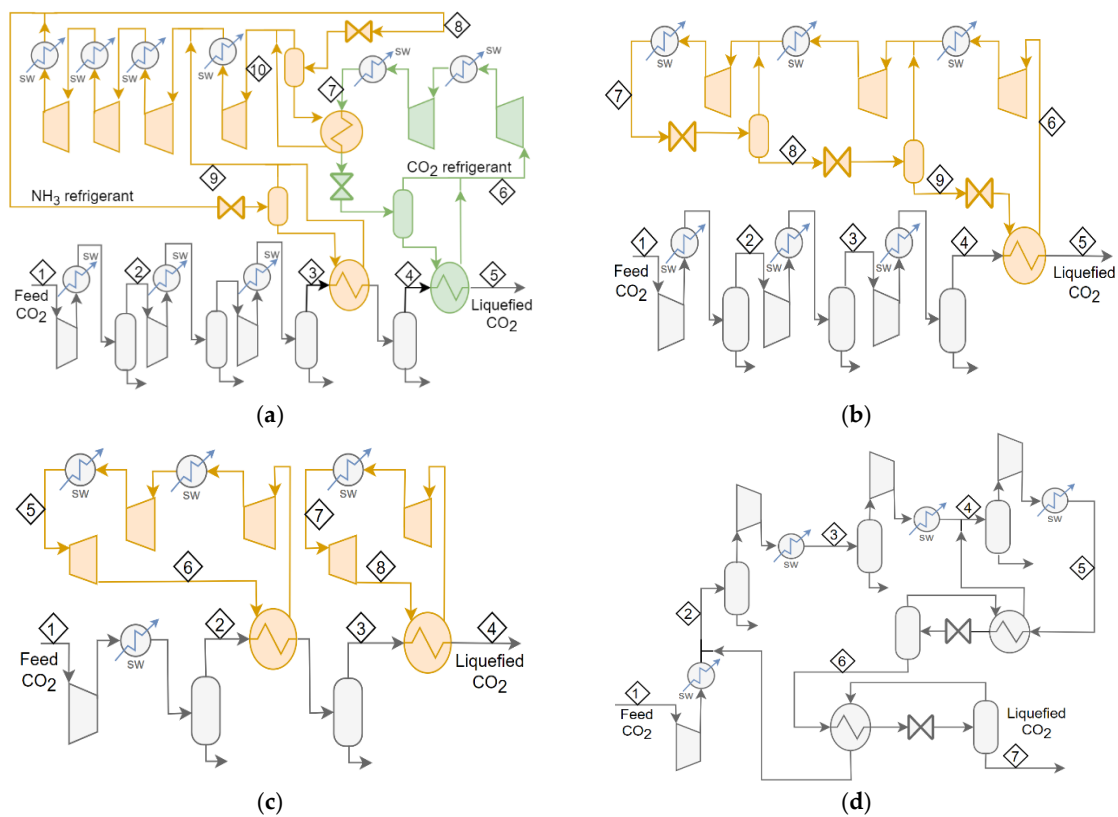


Figure 1. Process flow diagrams for the “base” cases for the CO₂ liquefaction schemes; (a) shows Case 1, (b) Case 2, (c) Case 3, and (d) Case 4.

Although each of these schemes was developed by the original study authors to achieve low energy consumption, each was developed based on a different set of modelling assumptions. A summary of the parameters used in each case is made below in Table 1.

Table 1. Summary of modelling parameters.

	Case 1	Case 2	Cases 3 and 4	“base”
Exchanger pressure drop, ΔP , (bara)	0.10	0.20	0.50 ²	0.30 ¹
Min. exchanger approach, ΔT_m , (°C)	3	3	5	5
Compressor efficiency (%)	80	75	85	85
Compressor stage limit	90 °C	Pr < 3	150 °C ¹	150 °C
Expander efficiency (%)	-	-	90	90
Cooling utility temp, ΔT_c , (°C)	35	35	15	25
CO ₂ feed pressure (bara)	1.8	1.8	0.20	0.10
CO ₂ feed temp (°C)	38 ¹	40	15 ¹	30
CO ₂ product pressure (bara)	8.0	15	7.0	15
CO ₂ temperature (°C)	-45	-28	-50	-28

¹ assumed, ² pressure drop for the refrigerant side of evaporator is zero bara.

To select a process scheme as the basis for this work, it was determined that the performance of each of the four “base” case schemes (Cases 1 to 4) should be compared on a consistent basis. This basis was selected based on a review of the range of the original operating parameters used in Cases 1 to 4. A review of the earlier work carried out by Jackson et al. [22] was also used to ensure compatibility with other related study work. The resulting “base” parameters are also summarized in Table 1.

Omitted from Table 1 is a summary of the CO₂ compositions used as the basis in each of the cases. This is partly for the sake of brevity and partly because the composition of the CO₂ stream used is not a focus of this study. For validation purposes, the CO₂ feed stream compositions used in Cases 1 to 4

corresponded to the original study basis; in all subsequent work a pure stream of CO₂ was used as the basis.

2.3. Process Modelling and Validation

A process model for each of the schemes was developed using Aspen HYSYS [23]. Operating conditions and energy flows were calculated using the Peng Robinson equation of state. Earlier studies have confirmed that the Peng Robinson equation of state generally provides reasonable accuracy in predicting the relevant properties for pure CO₂ apart from the region immediately around the critical point [24,25].

To validate the modelling approach the flow schemes shown in Figure 1 were recreated with the parameters used in their original development. Where modelling parameters could not be determined directly by reference to the published data, assumptions were made. In Case 1 the temperature out of the NH₂/CO₂ exchanger was unknown and was, therefore, selected in this work to provide minimum overall power. In the study data published for Case 2, the compressor stage pressure ratios are not reported and, therefore, in this work a constant pressure ratio (equal to 2.1) was assumed. In Case 3, the number of compressor stages used in the LP ammonia refrigeration is unclear and in this work two compression stages are used to limit maximum temperature to 150 °C.

The detailed modelling results for each of the four validation cases are presented in Appendix A and a summary of the reported and modelled energy consumption is presented below in Table 2, which shows good agreement between the reported and modelled values.

Table 2. Summary of the reported and modelled power consumptions for the “base” flow schemes.

	Case 1	Case 2	Case 3	Case 4
Modelled (kWh/ton)	106	101	79.9	86.6
Reported (kWh/ton)	104	102	80.3	87.0
Difference (%)	1.9	>1	>1	>1

It is worth noting that in Case 1, the energy consumption associated with pumping the CO₂ product up to 150 bara is included in the model validation work although this is not needed for liquefaction at low pressure.

2.4. Optimization and Comparison of the “Base” Schemes

To ensure a consistent basis for the comparison of the four “base” flow schemes, the fixed set of “base” parameters shown in Table 1 were used in each of the cases. To ensure that the comparison was a fair one, the variable operating parameters for each case were optimized to achieve the minimum energy consumption for each case.

2.4.1. Implications of the “Base” Parameters

Implementation of the “base” parameters shown in Table 1 in the “base” flow schemes for Cases 1 to 4 (illustrated in Figure 1) has an impact on the flow scheme design in some cases. In Case 1, a cooling temperature of 25 °C and a maximum temperature of 150 °C requires one fewer stages in each of the three compressors compared to the “base” flow scheme illustrated in Figure 1a. In Case 2, the CO₂ feed compressor also required one fewer stages for the 8.9 bara case compared to the scheme shown in Figure 1, but the NH₃ compressor remained unchanged compared to the original design. In Case 3, due to a lower CO₂ feed pressure, an extra stage is needed in the CO₂ feed compressor. The low-pressure NH₃ refrigeration compressors associated with Case 3 also require an additional stage to meet the 150 °C limit, but the high-pressure compressor is unchanged. In Case 4, the CO₂ feed compressor also needs an additional stage, but the scheme is otherwise unchanged. Each of these

modifications was implemented in the models developed for the “base” case flow schemes when making the comparisons of process performance for each case in this part of the study.

2.4.2. Optimization

The approach to optimization used in this study was to conduct the optimization outside of HYSYS using a link to MATLAB [26]. This link allowed the two-way transfer of process parameters between MATLAB and HYSYS and the implementation of the optimization algorithms directly in MATLAB.

The optimization algorithms used in MATLAB were *fminsearch* and GA. *fminsearch* uses a simplex algorithm that is suitable for unconstrained, multi-variable, non-linear optimization problems. A benefit of this method is that it will usually quickly converge to a solution; a downside is that in some cases a local minimum may be obtained. A drawback specific to the application of this algorithm in this study is that an unconstrained search can also lead HYSYS to non-viable solutions (e.g., where temperature crossing is inevitable in heat exchangers), which pauses the HYSYS solver and requires a time-consuming re-set of the optimization process. The GA algorithm can solve smooth or non-smooth optimization problems with or without constraints. It is a stochastic, population-based, algorithm, which is generally slower than *fminsearch* to reach a solution, but more reliable in solving the global minimum.

The objective of the optimization work was to minimize the energy consumption, which can be expressed as the sum of all compressor and expander stage energy consumptions:

$$\min f(P_i) = \sum W_{comp} - \sum W_{exp} \quad \text{for } i = 1, \dots, n, \quad (1)$$

where P_i is the compressor discharge pressure level that is optimized, W_{comp} is the compression stage energy flows (CO₂ and NH₃ compressor stages are not differentiated here), W_{exp} is the expander stage energy flows (only relevant where an expander forms part of the process scheme), and n is the number of variable pressure specifications, which varies from case-to-case, as described in more detail below.

In Case 1, the condensing pressure in the CO₂ refrigeration loop is set by the NH₃ refrigeration process and the evaporating pressure is set by the liquefaction process; the maximum pressure in the NH₃ refrigeration loop is set by the condensing temperature; and the discharge pressure from the first NH₃ compressor stage is set by the liquefaction process. This leaves the two remaining pressure levels in the NH₃ refrigeration compressor and the inter-stage pressure for the CO₂ feed compressor as variables that can be optimized, giving $n = 3$.

In Case 2, the pressure level used in the second and third stages of the NH₃ compressor are optimization variables along with the inter-stage pressure of the CO₂ feed compressor, also giving $n = 3$.

In Case 3, the inter-stage pressure of the low pressure NH₃ compressor is an optimization variable along with the inter-stage pressure of the CO₂ feed compressor, making $n = 2$.

In Case 4, the discharge pressure for each of the CO₂ compression stages is an optimization variable apart from the stage that occurs at the liquefaction pressure level, making $n = 4$.

When using the GA routine, the compressor stage outlet temperature was set as a constraint in the optimization algorithm for all cases:

$$T_i = f(P_i) \leq 150 \text{ }^\circ\text{C} \quad \text{for } i = 1, \dots, n, \quad (2)$$

where T_i is the temperature at each of the compressor discharge pressure levels that can be optimized. When *fminsearch* was used, T_i was checked manually and constrained, when necessary, by applying an appropriate constraint to an individual stage pressure level. Table 3 presents the results of the optimization work for the “base” process schemes (Cases 1 to 4).

Table 3. Summary of optimized power consumption for the base process schemes.

Case	Case 1	Case 2	Case 3	Case 4
Refrigerant	CO ₂ and NH ₃	NH ₃	NH ₃	CO ₂ -open
Cycle	cascade	3-stage	dual	2-stage
Cooling method	valves	valves	expanders	valves
Cooling stages	2-stage	1-stage	2-stage	n/a
Pressure (bara)	8.9 15	15	7.0 15	7.0 15
Energy (kWh/ton)	105 96.0	92.6	103 93.3	106 95.2

2.5. Development and Selection of the Study Basis

The performance comparisons made using the “base” parameters as shown in Table 1 allowed the best performing processes to be identified from Cases 1 to 4 using the methods described above. The comparisons also helped—in some cases—to identify the potential improvements in the flow schemes. In particular, the use of expanders in place of valves in Case 4 was identified as a potential improvement along with the possibility of an additional stage of cooling in Cases 2 and 4.

The application of these features in the flow schemes for Cases 1 to 4 leads to the development of five new cases. The new cases as called Case 4b, which is Case 4 with expanders replacing valves; Cases 5a and 5b, which are developed from Case 2 by adding an extra cooling stage (5a with valves and 4b with expanders); and Case 6, which is developed from Case 4 by adding an additional stage and valves or expanders. Figures 2 and 3 present the flow scheme for Cases 5 and 6.

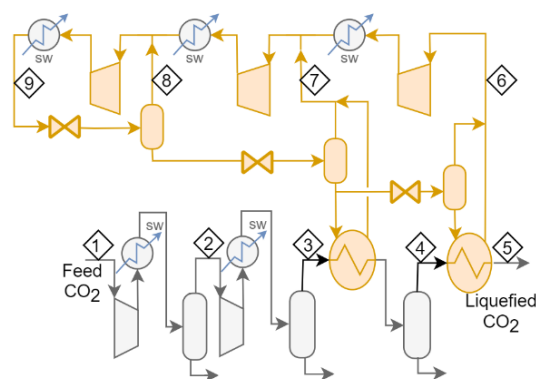


Figure 2. Flow scheme for Case 5a. In Case 5b, each of the three letdown valves is replaced with an expander.

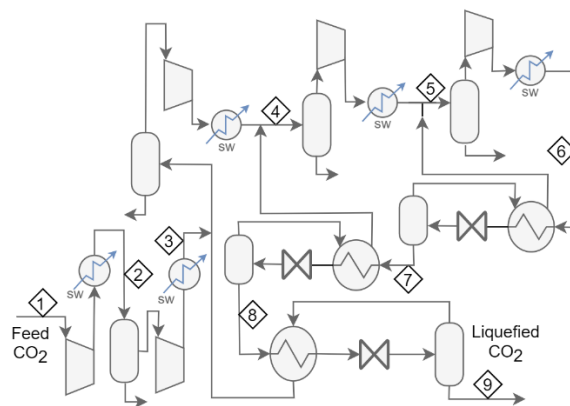


Figure 3. Flow scheme for Case 6a. In Case 6b, each of the three letdown valves is replaced with an expander.

Each of these new cases were optimized following the same procedure as Cases 1 to 4. The number of optimization variables, *n*, for Cases 5a and b are each less than Case 2 because the pressure level in

the second stage of the NH₃ compressor in Cases 5a and b is set by the temperature in the CO₂ cooler (i.e., just above 0 °C). This gives $n = 2$ for Cases 5a and 5b. Cases 6a and b have the same number of optimization variables as Case 4 ($n = 4$). Table 4 presents the results of the optimization work for Case 5 and Case 6.

Table 4. Summary of optimized power consumption for the new process schemes.

Case	Case 4b	Case 5a	Case 5b	Case 6a	Case 6b
Refrigerant	CO ₂ -open	NH ₃	NH ₃	CO ₂ -open	CO ₂ -open
Cycle	2-stage	3-stage	3-stage	3-stage	3-stage
Cooling method	expanders	valves	expanders	valves	expanders
Cooling stages	n/a	2-stage	2-stage	n/a	n/a
Pressure (bara)	15	15	15	15	15
Energy (kWh/ton)	89.5	91.8	90.8	93.0	88.7

Once the optimization process was complete, the best performing schemes were selected for the final part of the modelling work: the investigation of the impact of ambient temperature on energy consumption.

2.6. Performance Variation with Cooling Temperature

The method used to determine the Cases that would be studied in the final part of the modelling work was to first identify the best performing schemes and then second to consider what might represent the natural “next-best” process alternatives taking into consideration the complexity of each of the best performing cases. The selected cases were then optimized for temperatures in the range 15 to 50 °C aftercooler temperature.

3. Results

The main results of this study are presented below.

3.1. Process Modelling and Validation

The main results of the validation work, which are presented in the Method part of this paper, show that there is good agreement between the reference studies and the modelling work conducted here. As a supplement to this, the detailed modelling results for the validation cases are presented in Appendix A as Tables A1–A4. The stream numbering used corresponds to that shown in Figure 1.

3.2. Performance Comparisons

The energy consumption associated with each of the “base” process schemes (Cases 1 to 4) is presented below in Table 3. In all cases, the “base” operating parameters are used (see Table 1) and the values of all variable operating parameters are optimized to minimize energy consumption.

The results show that the 15 bara cases offer reduced power consumption in all of the “base” process schemes. They also show that a 3-stage NH₃ process has the potential to outperform a 2-stage expander-based process and that a 2-stage open CO₂ cycle can also offer low energy consumption. Based on these findings, Cases 4b, 5a, 5b, 6a, and 6b were developed. The performance of the optimized versions of these schemes is presented below in Table 4.

Table 4 shows that Case 6b offers lowest overall energy consumption when compared at 25 °C cooling temperature and that the use of expanders in the open CO₂ refrigeration cycle offers a significant benefit over the use of valves. In the case of the NH₃ refrigeration process, the benefit of using expanders is not as pronounced.

Based the results shown on Tables 3 and 4, three cases were selected for study in the next part of the work: Case 6b, because it offers the lowest overall power; Case 6a because it offers a more conventional alternative to Case 6b; and Case 5a to provide a comparison with a NH₃-based process. Case 5b was not

selected because the addition of expanders offered little reduction in energy consumption compared to Case 5a. The detailed modelling results for the cases shown in Tables 3 and 4 are presented in Appendix A.

3.3. Performance Variation with Cooling Temperature

Figure 4 shows how the energy consumption for Cases 5a, 6a, and 6b varies with ambient temperature. The smoothness of the three curves gives an indication of the level of consistency achieved in the optimization process. The results presented in Figure 4 illustrates the significant impact of cooling temperature on process performance and also, how at higher temperatures the performance of Case 5a improves relative to Cases 6a and 6b.

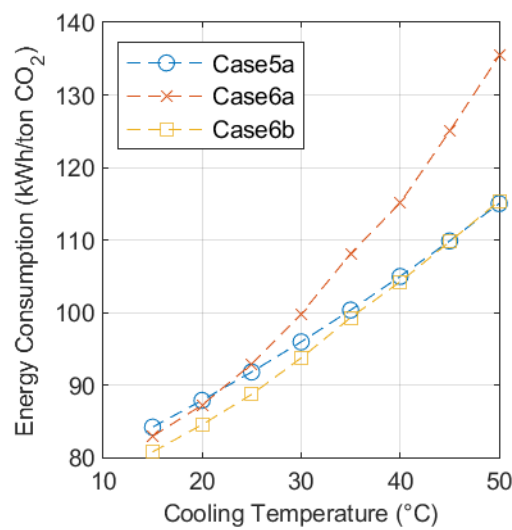


Figure 4. Variation in energy consumption for Cases 5a, 6a, and 6b with cooling temperature.

Figure 5 shows the variation in the operating pressure parameters for Cases 5a, 6a, and 6b. Again, the smoothness of the two curves gives an indication of the level of consistency achieved in the optimization process. In both cases, the inter-stage pressure of the CO₂ feed compressor drops as the cooling temperature increases. This is a result of the 150 °C temperature limits, which represents the optimum condition for inter-stage pressure in all the cases shown here.

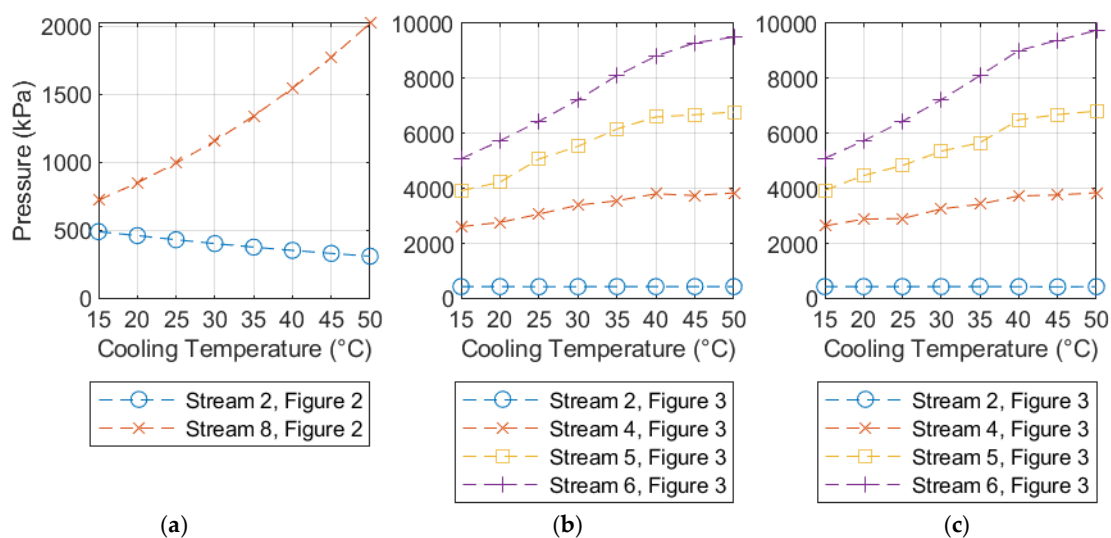


Figure 5. Variation in the optimization parameters for Cases 5a (a), 6a (b), and 6b (c).

4. Discussion

Table 2 shows that the modelling approach used in this study is validated by comparing the results with other similar studies. Additionally, the smoothness of the curves presented in Figures 4 and 5 shows that the optimization of the process parameters for Cases 5a, 6a, and 6b has been made on a consistent basis giving confidence in the trends illustrated in the results.

The variation of performance with ambient temperature presented in Figure 4 shows that Case 6a is the process that consumes the least energy across most of the temperature range studied. There is, however, a trade-off point around 45 °C, where Case 5a becomes the lowest energy consuming case. Case 6a does not offer the minimum energy consumption in any cases, but it does outperform Case 5a when the cooling temperature is below 20 °C. These trends support the original assertion of Hegerland [6] that open-cycle CO₂-based systems outperform NH₃-based refrigeration at low temperatures.

It is worth noting that the comparison between Case 5a and 6b is not entirely a fair one since the machinery required in Case 6b is significantly more complicated than that required in Case 5a. The potential benefit of a turbo expander-based process would ultimately be determined by the optimum balance between operating and capital costs, which in-turn will vary between projects. Also worth noting is that Case 4b offers similar performance to Case 6b with a small reduction in process complexity. Although the life-cycle costing of these schemes falls outside the scope of this study, the results provided here suggest that all of the Cases 4b, 5a, 6a, and 6b would merit consideration in a techno-economic study of the CO₂ liquefaction process.

Cases 5a and 6a could be considered “conventional” and are also similar in the level of process complexity involved. Case 6a does, however, have a potentially significant advantage over Case 5a because of the possibility of condensing water out of the CO₂ stream at pressure levels above the final liquefaction pressure. This will reduce, and possibly eliminate, the requirement for an additional dehydration step in the process. Therefore, in Case 5a an additional pressure-drop associated with a dehydration unit located prior to the liquefaction step may be necessary, representing a small additional energy penalty for this process. Again, the level of dehydration required and the energy penalty this represents would be expected to vary on a project-by-project basis.

5. Conclusions

As suggested by Hegerland [6] the energy consumption of open CO₂-based refrigeration processes is found in this study to be lower than NH₃-based refrigeration alternatives when ambient temperature is low. This study finds that the trade-off temperature also varies with the complexity of the specific processes considered: Case 6a has a trade-off point with Case 5a at a cooling temperature of 20 °C, whereas the more complex Case 6b has a trade off with 5a at 45 °C. The cooling temperature is also found to strongly influence the minimum energy consumption, which rises by around 40% for Cases 5a and 6b over the range 15 to 50 °C and by around 60% for Case 6a. This variation in energy consumption could be expected to be important for the accurate development of CCUS system models and the determination of the trade-off point between shipping and pipelines where the potential sources on disposal locations lie in locations with different ambient temperature conditions.

Author Contributions: Conceptualization, S.J.; Methodology, S.J. and E.B.; Validation, S.J.; Formal analysis, S.J.; Investigation, S.J.; Resources, S.J.; Data curation, S.J.; Writing—original draft preparation, S.J.; Writing—review and editing, S.J. and E.B.; Supervision, E.B.

Funding: This research received no external funding.

Conflicts of Interest: The authors declare no conflict of interest.

Appendix A

Appendix A.1. Detailed Modelling Results for the Validation Cases

Table A1. Mass balance for the Case 1 verification model, numbering as Figure 1a.

Case 1	1	2	3	4	5	6	7	8	9	10
Temperature (°C)	38.0	38.0	38.0	1.00	−45.1	38	−48.1	38	−2.7	−16
Pressure (bara)	1.8	3.1	8.2	8.1	8.0	23.9	7.1	14.6	3.8	2.2
Flow (ton/h)	80.5	73.1	72.7	72.5	72.5	103.0	103	31.3	2.8	31.3

Table A2. Mass balance for the Case 2 verification model, numbering as Figure 1b.

Case 2	1	2	3	4	5	6	7	8	9
Temperature (°C)	35	35	35	35	−28	−36.7	35	7.80	−15.2
Pressure (bara)	1.8	3.6	7.3	15	15	0.83	13.4	5.6	2.3
Flow (ton/h)	114	114	114	114	114	32.2	39.2	35.0	32.2

Table A3. Mass balance for the Case 3 verification model, numbering as Figure 1c.

Case 3	1	2	3	4	5	6	7	8
Temperature (°C)	20	15	1.0	−50	15	−55	15	−4.0
Pressure (bara)	2.0	8.0	7.5	7.0	7.2	0.30	7.2	3.6
Flow (ton/h)	125	122	122	122	40.8	40.8	1.36	1.36

Table A4. Mass balance for the Case 4 verification model, numbering as Figure 1d.

Case 4	1	2	3	4	5	6	7
Temperature (°C)	20	10	15	14.4	15	3.7	−48.5
Pressure (bara)	2.0	6.5	11.5	37.5	70.0	38.0	7.0
Flow (ton/h)	125	177	177	200	200	176	122

Appendix A.2. Detailed Modelling Results for Optimised Base Cases

Table A5. Mass balance Case 1, 15 bara liquefaction pressure, stream numbering from Figure 1.

Case 1 (15 Bara)	1	2	3	4	5	6	7	8	9	10
Temperature (°C)	25.0	25.0	25.0	1.0	−27.7	−30.7	25.0	25.0	−2.0	−10.0
Pressure (bara)	1.00	4.01	15.6	15.3	15.0	13.6	28.7	9.95	3.94	2.87
Flow (ton/h)	100	100	100	100	100	130	130	33.0	1.96	33.0

Table A6. Mass balance Case 2, 15 bara liquefaction pressure, stream numbering from Figure 1.

Case 1 (15 Bara)	1	2	3	4	5	6	7	8	9
Temperature (°C)	25.0	25.0	-	25.0	−27.7	−32.7	25.0	13.0	−1.48
Pressure (bara)	1.00	4.01	-	15.30	15.00	1.03	9.95	6.74	4.01
Flow (ton/h)	100	100	-	100	100	28.7	31.8	30.3	28.7

Table A7. Mass balance Case 3, 15 bara liquefaction pressure, stream numbering from Figure 1.

Case 1 (15 Bara)	1	2	3	4	5	6	7	8
Temperature (°C)	25.0	25.0	1.0	−27.7	25.0	−3.96	25.0	−32.7
Pressure (bara)	1.00	15.6	15.3	15.0	9.95	3.65	9.95	1.03
Flow (ton/h)	100	100	100	100	1.96	1.96	29.2	29.2

Table A8. Mass balance Case 4, 15 bara liquefaction pressure, stream numbering from Figure 1.

Case 1 (15 Bara)	1	2	3	4	5	6	7
Temperature (°C)	25.0	19.3	25.0	23.6	25.0	9.44	−27.7
Pressure (bara)	1.00	14.7	27.8	43.9	65.0	44.2	15.0
Flow (ton/h)	100	138	138	191	191	138	99.3

Appendix A.3. Detailed Modelling Results for New Cases

Table A9. Mass balance for Case 4b, stream numbering from Figure 1.

Case 4b	1	2	3	4	5	6	7
Temperature (°C)	25.0	19.8	25.0	23.7	25.0	10.2	−27.7
Pressure (bara)	1.00	14.7	28.0	44.7	65.0	45.0	15.0
Flow (ton/h)	100	135	135	182	182	134	100

Table A10. Mass balance for Case 5a, stream numbering from Figure 2.

Case 5a	1	2	3	4	5	6	7	8	9
Temperature (°C)	25.0	25.0	25.0	1.00	−27.7	−32.7	2.11	12.9	25.0
Pressure (bara)	1.00	4.01	15.6	15.3	15.0	1.03	3.94	6.73	9.95
Flow (ton/h)	100	100	100	100	100	26.8	3.39	1.51	31.7

Table A11. Mass balance for Case 5b, stream numbering from Figure 2.

Case 5b	1	2	3	4	5	6	7	8	9
Temperature (°C)	25.0	25.0	25.0	1.00	−27.7	−32.7	1.89	15.0	25.0
Pressure (bara)	1.00	4.01	15.6	15.3	15.0	1.03	3.93	7.22	9.95
Flow (ton/h)	100	100	100	100	100	26.6	3.57	1.25	31.4

Table A12. Mass balance for Case 6a, stream numbering from Figure 3.

Case 6a	1	2	3	4	5	6	7	8
Temperature (°C)	25.0	19.2	21.5	23.7	25.0	13.4	−5.5	−27.7
Pressure (bara)	1.00	14.7	29.3	48.5	64.4	48.8	29.6	15.0
Flow (ton/h)	100	119	151	201	201	152	121	102

Table A13. Mass balance for Case 6b, stream numbering from Figure 3.

Case 6b	1	2	3	4	5	6	7	8
Temperature (°C)	25.0	19.6	21.6	23.8	25.0	13.2	−5.9	−27.7
Pressure (bara)	1.00	14.7	29.0	48.3	64.4	48.6	29.3	15.0
Flow (ton/h)	100	118	146	192	192	146	118	100

References

1. Norhasyima, R.S.; Mahlia, T.M.I. Advances in CO₂ utilization technology: A patent landscape review. *J. CO₂ Util.* **2018**, *26*, 323–335. [[CrossRef](#)]
2. Eide, L.I.; Batum, M.; Dixon, T.; Elamin, Z.; Graue, A.; Hagen, S.; Hovorka, S.; Nazarian, B.; Nøkleby, P.H.; Olsen, G.I.; et al. Enabling large-scale carbon capture, utilisation, and storage (CCUS) using offshore carbon dioxide (CO₂) infrastructure developments—A review. *Energies* **2019**, *12*, 1945. [[CrossRef](#)]
3. Edwards, R.W.J.; Celia, M.A. Infrastructure to enable deployment of carbon capture, utilization, and storage in the United States. *Proc. Natl. Acad. Sci. USA* **2018**, *115*, E8815–E8824. [[CrossRef](#)] [[PubMed](#)]
4. Peletiri, S.P.; Rahmanian, N.; Mujtaba, I.M. CO₂ Pipeline design: A review. *Energies* **2018**, *11*, 2184. [[CrossRef](#)]

5. Metz, B.; Davidson, O.; De Coninck, H.; Loos, M.; Meyer, L. *Carbon Dioxide Capture and Storage*; IPCC, 2005: IPCC Special Report on Carbon Dioxide Capture and Storage; Cambridge University Press: Cambridge, UK, 2005.
6. Hegerland, G.; Jørgensen, T.; Pande, J.O. Liquefaction and handling of large amounts of CO₂ for EOR. In *Greenhouse Gas Control Technologies 7*; Elsevier Science Ltd.: Amsterdam, The Netherlands, 2005; pp. 2541–2544.
7. Mallon, W.; Buit, L.; van Wingerden, J.; Lemmens, H.; Eldrup, N.H. Costs of CO₂ Transportation Infrastructures. *Energy Procedia* **2013**, *37*, 2969–2980. [[CrossRef](#)]
8. Jakobsen, J.; Roussanaly, S.; Anantharaman, R. A techno-economic case study of CO₂ capture, transport and storage chain from a cement plant in Norway. *J. Clean. Prod.* **2017**, *144*, 523–539. [[CrossRef](#)]
9. Mitsubishi Heavy Industries Ltd. *Ship Transport of CO₂*; PH4/30; IEA Greenhouse Gas R&D Programme: Cheltenham, UK, 2004.
10. Jordal, K.; Aspelund, A. Gas conditioning—The interface between CO₂ capture and transport. *Int. J. Greenh. Gas Control* **2007**, *1*, 343–354.
11. Roussanaly, S.; Brunsvold, A.L.; Hognes, E.S. Benchmarking of CO₂ transport technologies: Part II—Offshore pipeline and shipping to an offshore site. *Int. J. Greenh. Gas Control* **2014**, *28*, 283–299. [[CrossRef](#)]
12. Duan, L.; Chen, X.; Yang, Y. Study on a novel process for CO₂ compression and liquefaction integrated with the refrigeration process. *Int. J. Energy Res.* **2013**, *37*, 1453–1464. [[CrossRef](#)]
13. Alabdulkarem, A.; Hwang, Y.H.; Radermacher, R. Development of CO₂ liquefaction cycles for CO₂ sequestration. *Appl. Therm. Eng.* **2012**, *33–34*, 144–156. [[CrossRef](#)]
14. Øi, L.E.; Eldrup, N.H.; Adhikari, U.; Bentsen, M.H.; Badalge, J.C.L.; Yang, S. Simulation and Cost Comparison of CO₂ Liquefaction. *Energy Procedia* **2016**, *86*, 500–510. [[CrossRef](#)]
15. Aspelund, A.; Mølnvik, M.J.; De Koeijer, G. Ship Transport of CO₂: Technical Solutions and Analysis of Costs, Energy Utilization, Exergy Efficiency and CO₂ Emissions. *Chem. Eng. Res. Des.* **2006**, *84*, 847–855. [[CrossRef](#)]
16. Lee, U.; Yang, S.; Jeong, Y.; Lim, Y.; Lee, C.S.; Han, C. Carbon Dioxide Liquefaction Process for Ship Transportation. *Ind. Eng. Chem. Res.* **2012**, *51*, 15122–15131. [[CrossRef](#)]
17. Decarre, S.; Berthiaud, J.; Butin, N.; Guillaume-Combecave, J. CO₂ maritime transportation. *Int. J. Greenh. Gas Control* **2010**, *4*, 857–864. [[CrossRef](#)]
18. Seo, Y.; Huh, C.; Lee, S.; Chang, D. Comparison of CO₂ liquefaction pressures for ship-based carbon capture and storage (CCS) chain. *Int. J. Greenh. Gas Control* **2016**, *52*, 1–12. [[CrossRef](#)]
19. Seo, Y.; You, H.; Lee, S.; Huh, C.; Chang, D. Evaluation of CO₂ liquefaction processes for ship-based carbon capture and storage (CCS) in terms of life cycle cost (LCC) considering availability. *Int. J. Greenh. Gas Control* **2015**, *35*, 1–12. [[CrossRef](#)]
20. Jackson, S.; Brodal, E. *A Comparison of the Energy Consumption for CO₂ Compression Process Alternatives*; IOP Conference Series: Earth and Environmental Science; IOP Publishing: Bristol, UK, 2018.
21. Lee, S.G.; Choi, G.B.; Lee, J.M. Optimal Design and Operating Conditions of the CO₂ Liquefaction Process, Considering Variations in Cooling Water Temperature. *Ind. Eng. Chem. Res.* **2015**, *54*, 12855–12866. [[CrossRef](#)]
22. Jackson, S.; Brodal, E. Optimization of the Energy Consumption of a Carbon Capture and Sequestration Related Carbon Dioxide Compression Processes. *Energies* **2019**, *12*, 1603. [[CrossRef](#)]
23. *HYSYS v9*; AspenTech: Bedford, MA, USA.
24. Mazzocoli, M.; Bosio, B.; Arato, E.; Brandani, S. Comparison of equations-of-state with P-p-T experimental data of binary mixtures rich in CO₂ under the conditions of pipeline transport. *J. Supercrit. Fluids* **2014**, *95*, 474–490. [[CrossRef](#)]
25. Wilhelmsena, Ø.; Skaugena, G.; Jørstadb, O.; Hailong, L. Evaluation of SPUNG# and other Equations of State for use in Carbon Capture and Storage modelling. *Energy Procedia* **2012**, *23*, 236–245.
26. *MATLAB*; The MathWorks Inc.: Natick, MA, USA, 2018.

